DOI: 10.1534/genetics.109.113357

The *Psychedelic* Genes of Maize Redundantly Promote Carbohydrate Export From Leaves

Thomas L. Slewinski and David M. Braun[1]

Department of Biology, Pennsylvania State University, University Park, Pennsylvania 16802

Manuscript received December 19, 2009
Accepted for publication February 6, 2010

ABSTRACT

Whole-plant carbohydrate partitioning involves the assimilation of carbon in leaves and its translocation to nonphotosynthetic tissues. This process is fundamental to plant growth and development, but its regulation is poorly understood. To identify genes controlling carbohydrate partitioning, we isolated mutants that are defective in exporting fixed carbon from leaves. Here we describe *psychedelic (psc)*, a new mutant of maize (*Zea mays*) that is perturbed in carbohydrate partitioning. *psc* mutants exhibit stable, discrete chlorotic and green regions within their leaves. *psc* chlorotic tissues hyperaccumulate starch and soluble sugars, while *psc* green tissues appear comparable to wild-type leaves. The *psc* chlorotic and green tissue boundaries are usually delineated by larger veins, suggesting that translocation of a mobile compound through the veins may influence the tissue phenotype. *psc* mutants display altered biomass partitioning, which is consistent with reduced carbohydrate export from leaves to developing tissues. We determined that the *psc* mutation is unlinked to previously characterized maize leaf carbohydrate hyperaccumulation mutants. Additionally, we found that the *psc* mutant phenotype is inherited as a recessive, duplicate-factor trait in some inbred lines. Genetic analyses with other maize mutants with variegated leaves and impaired carbohydrate partitioning suggest that *Psc* defines an independent pathway. Therefore, investigations into the *psc* mutation have uncovered two previously unknown genes that redundantly function to regulate carbohydrate partitioning in maize.

CARBON fixation and utilization underpin all aspects of plant biology. Carbon fixed in the photosynthetic tissues must be properly sensed, translocated, allocated, and utilized to ensure proper growth, development, and reproduction. When any one aspect of carbohydrate partitioning is disrupted, yield is usually affected (Moore *et al.* 2003; Lu and Sharkey 2004; Niittyla *et al.* 2004; Srivastava *et al.* 2008). Selective breeding has led to crop domestication and yield improvements, but the pathways responsible for these modifications in the context of carbon partitioning have not been well characterized (Whitt *et al.* 2002). The regulation of carbon partitioning in plants is likely to be complex and encompass multiple steps, including allocation into soluble sugars *vs.* insoluble starch, use for cellular metabolism *vs.* sugar export, and local utilization for organ growth *vs.* long-distance partitioning to sustain nonphotosynthetic tissues (Wardlaw 1990; Cheng *et al.* 1996; Koch 1996; Hannah 2005; Zeeman *et al.* 2007; Braun and Slewinski 2009). However, little is known about the control of whole-plant carbohydrate partitioning or the signal transduction pathways regulating sucrose transport across cellular membranes (Chiou and Bush 1998; Lalonde *et al.* 2004; Turgeon 2006; Sauer 2007; Smith and Stitt 2007; Slewinski and Braun 2010).

Maize is a well-established model organism for studies of carbon physiology and sucrose transport in plants (Evert *et al.* 1978; Heyser *et al.* 1978; Evert 1980; Heyser 1980; Kalt-Torres *et al.* 1987; Nolte and Koch 1993; Slewinski *et al.* 2009). Although the pathway for carbon movement in maize leaves has been studied for more than 40 years, little is known about its regulation (Hofstra and Nelson 1969; Braun and Slewinski 2009). Maize leaves contain three orders of longitudinal veins: large, intermediate, and small. The different vein types have distinct functions in carbohydrate partitioning and can be distinguished anatomically (Russell and Evert 1985). Large veins contain metaxylem vessels and hypodermal sclerenchyma that connect the vein to both the adaxial and abaxial epidermis. Intermediate veins lack metaxylem vessels but contain hypodermal sclerenchyma subtending one or both epidermal surfaces. Small veins lack metaxylem vessels and hypodermal sclerenchyma. Small and intermediate veins, collectively referred to as minor veins, primarily function in sucrose uptake into the phloem from the photosynthetic cells (Fritz *et al.* 1983) and

Supporting information is available online at http://www.genetics.org/cgi/content/full/genetics.109.113357/DC1.

[1]*Corresponding author:* 208 Mueller Lab, Department of Biology, Pennsylvania State University, University Park, PA 16802.
E-mail: dbraun@psu.edu

intergrade into the large veins toward the base of the leaf blade (Russell and Evert 1985). In contrast, the large veins are principally involved in long-distance transport (Fritz *et al.* 1989).

Maize utilizes C_4 carbon assimilation and displays Kranz anatomy in its leaves: mesophyll cells encircle bundle sheath cells, which in turn surround the vein (Esau 1977; Edwards *et al.* 2001). Sucrose, the translocated form of carbohydrate, is synthesized in the mesophyll cells (Lunn and Furbank 1999) and diffuses symplastically through plasmodesmata, intercellular channels connecting adjacent plant cells, into the bundle sheath cells and then into the vascular parenchyma cells (Russin *et al.* 1996). By an unknown mechanism, sucrose is transported out of the vascular parenchyma cells into the apoplast (Evert *et al.* 1978; Heyser 1980; Slewinski *et al.* 2009). Sucrose transporters located in the plasma membrane of companion cells and/or sieve elements import sucrose from the apoplast, actively concentrating it within phloem tissue for long-distance transport to other parts of the plant (Lalonde *et al.* 2004; Sauer 2007).

Characterization of mutants that display abnormalities in carbohydrate partitioning represents one approach to identifying genes that function in this process. To date, only four maize mutants that hyperaccumulate carbohydrates within their leaves and that function independently of starch metabolism have been reported: *sucrose export defective1* (*sxd1*), *tie-dyed1* (*tdy1*), *tie-dyed2* (*tdy2*), and *sucrose transporter1* (*sut1*) (Russin *et al.* 1996; Blauth *et al.* 2001; Provencher *et al.* 2001; Dinges *et al.* 2003; Braun *et al.* 2006; Baker and Braun 2008; Slewinski *et al.* 2008, 2009). *sut1* mutant leaves are uniformly chlorotic, whereas the other three mutants are unique in that they form both normal-appearing green and chlorotic leaf regions, the latter of which hyperaccumulate starch and soluble sugars. All four mutants hyperaccumulate starch in both the bundle sheath and mesophyll cells, whereas wild-type plants normally contain starch only in the bundle sheath cells (Rhoades and Carvalho 1944). Additionally, all four mutants show reduced plant stature, delayed reproductive maturity, and diminished reproductive tissues. Retention of carbohydrates in chlorotic leaf tissues is thought to cause these phenotypes.

Although variegated, the *sxd1* mutant phenotype differs from the *tdy* mutants. *sxd1* mutant phenotypic expression begins at the leaf tip and progressively spreads to the base as the leaf ages (Russin *et al.* 1996; Provencher *et al.* 2001). *Sxd1* encodes tocopherol cyclase, which functions in vitamin E biosynthesis (Sattler *et al.* 2003). Vitamin E deficiency leads to ectopic callose deposition, which occludes plasmodesmata specifically at the bundle sheath-vascular parenchyma cell interface, thus blocking symplastic sucrose transport upstream of sucrose release into the apoplast (Russin *et al.* 1996; Botha *et al.* 2000).

In contrast to *sxd1* mutants, the variegation pattern in *tdy* mutant leaves becomes visible upon leaf emergence from the whorl and remains fixed throughout the life of the leaf (Braun *et al.* 2006; Baker and Braun 2008). *tdy* mutant leaves develop large, nonclonal, chlorotic regions that violate cell lineage patterns of maize leaf development (Poethig and Szymkowiak 1995; Braun *et al.* 2006; Baker and Braun 2007, 2008). Hence, it was proposed that the *Tdy* genes may function as regulators of carbon flux rather than being directly involved in carbohydrate metabolism or transport (Braun *et al.* 2006; Baker and Braun 2008). A threshold model was hypothesized to explain the leaf variegation in *tdy* mutants: accumulation of a chloroplast byproduct, likely sucrose, above a threshold level induces the formation of a chlorotic tissue phenotype, while quantities below the threshold result in a normal-appearing green leaf region (Braun *et al.* 2006; Baker and Braun 2008).

Although in many ways the *tdy* mutant phenotypes are similar to those of *sxd1*, recent work determined that both *Tdy1* and *Tdy2* function independently of the *Sxd1* pathway (Baker and Braun 2008; Ma *et al.* 2008). Furthermore, genetic analyses suggest that the two *Tdy* genes function in the same pathway (Baker and Braun 2008). *Tdy1* encodes a novel, phloem-expressed, predicted transmembrane protein (Ma *et al.* 2009). The molecular identity of *Tdy2* is not known.

To gain insight into additional genetic regulators of carbon flux and allocation, we have identified many new loci controlling carbohydrate partitioning in maize leaves from a large collection of variegated, chlorotic mutants. Here, we characterize the *psychedelic* (*psc*) mutant, named because of the unique pattern of chlorotic and green leaf variegation reminiscent of the fabrics and art associated with the "hippie" movement of the 1960s. *psc* mutants display stable, nonclonal, chlorotic, and green regions within leaf tissues. *psc* green tissue is comparable to wild-type green tissue, whereas *psc* chlorotic tissue hyperaccumulates starch and soluble sugars. To investigate the role *Psc* plays in controlling carbohydrate accumulation in maize leaves, we characterized the *psc* mutant phenotype and performed genetic analyses to determine whether *Psc* functions independently of the previously identified maize genes regulating carbohydrate partitioning.

MATERIALS AND METHODS

Growth conditions and genetic stocks: Maize plants were grown under high-light conditions at the Pennsylvania State University Rock Springs Agronomy Farm during the summers of 2008 and 2009. Plants used for low-light experiments were grown in a shaded greenhouse in 400 μmol m^{-2} sec^{-1} light under a 12-hr day (30°) and 12-hr night (20°). The *psc-Reference* (hereafter *psc*) mutation arose spontaneously in a B73 inbred line. For phenotypic analyses, segregating 1:1 *psc*:wild-type families were generated by fertilizing heterozygous wild-type

plants with pollen from homozygous *psc* mutant siblings. Complementation tests were performed by crossing *psc* mutant plants in the B73 background to homozygous *tdy1-R*, *tdy2-R*, and *sxd1-1* mutant individuals introgressed six or more times into the B73 background. The F_1 plants were self-fertilized to produce segregating F_2 populations. At least two independent families were characterized for each of the double mutant analyses.

Starch staining and microscopy: Starch was visualized by clearing leaf tissue in boiling 95% ethanol and staining with iodine potassium iodide (IKI) solution (Ruzin 1999). Free-hand leaf cross-sections were examined under bright-field and UV light using a Nikon Eclipse 80i fluorescent microscope with a 100-W mercury lamp as described (Baker and Braun 2007). Aniline blue staining of callose was performed according to Ma *et al.* (2008).

Carbohydrate quantification: Carbohydrates were quantified according to Stitt *et al.* (1989). A total of 100 mg of tissue was collected between 5 and 6 pm on a sunny, cloudless day from leaves 15 and 16 on mature plants in mid-July 2008. Six biological replicates were conducted for each tissue type and the entire experiment was repeated three times with similar results. Data from a representative repeat are shown.

Photosynthetic, stomatal conductance and chlorophyll measurements: Photosynthetic and stomatal conductance measurements were taken on fully expanded leaves 15 and 16 from mature plants grown in the field in midsummer between 2 and 4 pm using a LICOR 6400 photosynthesis system as described (Huang *et al.* 2009). Six biological replicates were performed for each tissue type and the entire experiment was repeated three times. Data from a representative repeat are shown. Total chlorophyll levels were measured with a SPAD 502 data logger on leaves 15 and 16 from mature plants. A total of 25 biological replicates were performed for each tissue type and the experiment was repeated three times. Data from a representative repeat are shown.

Morphometric analyses: Morphometric analyses were done as described (Braun *et al.* 2006; Baker and Braun 2007; Ma *et al.* 2008). $N = 12$ for all parameters unless noted otherwise in figure legends and replicates were collected from two segregating families grown in separate field locations in the summer of 2008.

RESULTS

Identification of a new variegated maize mutant with starch hyperaccumulation in leaves: To identify additional genes controlling carbohydrate partitioning, we screened for mutants with phenotypes that resembled the *tdy* mutants. A spontaneous mutation arose in a B73 inbred line and was found to produce stable, nonclonal, variegated chlorotic leaf tissues (Figure 1, A and C). The stable, nonclonal phenotype indicated that the mutation is not caused by transposable element insertion or excision (Poethig and Szymkowiak 1995; Braun *et al.* 2006). The new mutant phenotype differed subtly from the *tdy* or *sxd1* mutant phenotypes in that the chlorotic regions appeared to be more longitudinally streaked and more likely to be localized toward the leaf margins (Figure 1C). To assess whether the chlorotic regions contained excess carbohydrates, we stained mutant and wild-type leaves with IKI at the end of the night. Wild-type leaves contained little starch, as indicated by the pale yellow color of the tissue (Figure 1B). However, the mutant leaves contained abundant starch within the chlorotic regions, as evidenced by the dark brown coloration (Figure 1D). The green regions of mutant leaves did not appear to contain elevated starch contents. Therefore, the chlorotic leaf regions, like those in the *tdy* and *sxd1* mutants, hyperaccumulated starch.

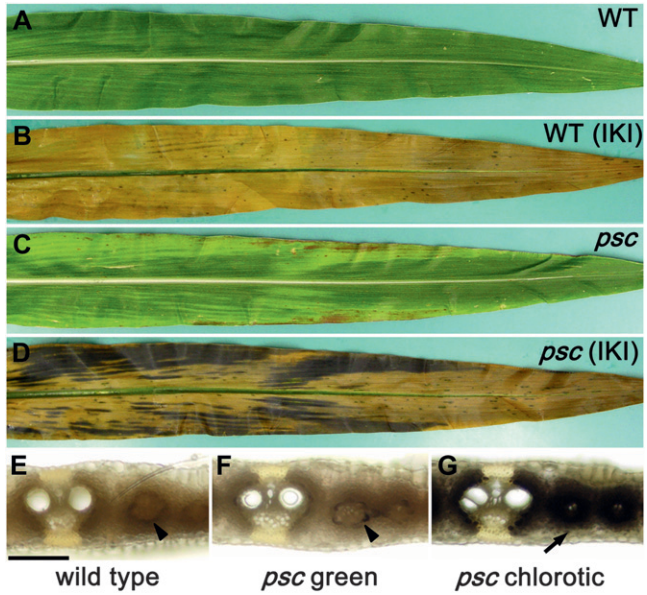

Figure 1.—*psc* leaves display chlorotic regions that hyperaccumulate starch. (A) Wild-type (WT) leaves have uniform green coloration. (B) Wild-type leaves cleared and IKI stained showing that the leaf contains little starch after the dark period. (C) *psc* leaves display chlorotic and green tissues. (D) *psc* leaves cleared and IKI stained showing that chlorotic regions hyperaccumulate starch after the dark period, whereas green regions do not. Free-hand leaf cross-sections of (E) wild-type, (F) *psc* green, and (G) *psc* chlorotic tissues. *psc* chlorotic tissue hyperaccumulates starch in both the bundle sheath and mesophyll cells (arrow in G), whereas wild-type and *psc* green tissues contain trace amounts of starch in the bundle sheath cells (arrowheads in E and F) after the dark period. Bar, 100 μm for panels E–G.

To determine which photosynthetic cells accumulated excess starch in the mutant, histological analysis was performed. In wild-type leaves, at the end of the night, trace amounts of starch were present only in the bundle sheath cells (Figure 1E). Green tissue from mutant leaves showed a similar pattern and level of starch deposition (Figure 1F). However, in the mutant chlorotic leaf tissue, large quantities of starch were observed in both the bundle sheath and mesophyll cells (Figure 1G). Hence, the starch accumulation pattern within the chlorotic tissues of the new mutant was similar to the *tdy* and *sxd1* mutants (Russin *et al.* 1996; Braun *et al.* 2006; Baker and Braun 2008).

To investigate whether the new mutation might be a new allele of *tdy1*, *tdy2*, or *sxd1*, we performed complementation crosses. In all cases, the F_1 appeared normal, and the mutants complemented each other. These data,

TABLE 1

***psc* displays single-factor recessive inheritance in the B73 inbred line**

Family no.	No. of mutants	No. of wild type	Total no.	% mutant
1	6	21	27	22.2[a]
2	8	30	38	21.1[a]
3	5	23	28	17.9[a]
4	16	39	55	29.1[a]
5	13	36	49	26.5[a]
6	11	41	52	21.2[a]
Total	59	190	249	23.7[a]

[a] χ^2 values fail to reject the null hypothesis of a 3:1 segregation ratio.

along with genetic analyses (see below), suggested that the new mutation represented a distinct locus, which we named *psychedelic* (*psc*) on the basis of its variegated appearance.

The *psc* phenotype displays duplicate-factor inheritance in some genetic backgrounds: To characterize the inheritance of the *psc* trait, wild-type heterozygous siblings were self-pollinated. The *psc* phenotype segregated one mutant to three wild type in the progeny, suggesting a single recessive mutation in the B73 background (Table 1). However, this result differed in other genetic backgrounds. *psc* phenotypic individuals from the B73 line were crossed to the Mo17 inbred line and self-pollinated. Interestingly, the F_2 generation segregated the *psc* mutant phenotype in a 1:15 ratio, suggesting duplicate-factor recessive inheritance (Table 2). To test this hypothesis, the F_1 plants were backcrossed to the *psc* mutant in B73. The F_2 progeny segregated *psc* mutants in a 1:3 ratio rather than a 1:1 ratio, supporting duplicate-factor inheritance (Table 2). Similar results were obtained when the same backcrossing scheme was performed with the W22 and A188 inbred lines (Table 2). These data indicate that the B73 inbred line is homozygous mutant for one of the unlinked *psc* duplicate loci, whereas the other inbred lines tested, each carry two functionally redundant genes.

Soluble sugars hyperaccumulate in *psc* chlorotic regions and are associated with decreased photosynthesis: To examine whether soluble sugars hyperaccumulated within *psc* leaves, we quantified their levels in leaves that were harvested at the end of the day, when carbohydrate contents peak. Green tissue in *psc* leaves had carbohydrate levels similar to wild type (Table 3). However, soluble sugars (sucrose, glucose, and fructose) and starch amounts were significantly increased in the *psc* chlorotic regions (Table 3). These data indicate that the carbohydrate partitioning defect in *psc* was not exclusive to starch, but also affected soluble sugars.

TABLE 2

***psc* displays duplicate-factor recessive inheritance in the Mo17, A188, and W22 inbred lines**

Family no.	Female parent	Male parent	No. of mutants	No. of wild type	Total no.	% mutant
1	*psc*(B73) × Mo17	Self-pollinated	6	111	117	5.1[a]
2	*psc*(B73) × Mo17	Self-pollinated	12	158	170	7.1[a]
3	*psc*(B73) × Mo17	Self-pollinated	5	105	110	4.5[a]
4	*psc*(B73) × Mo17	Self-pollinated	7	116	123	5.7[a]
5	*psc*(B73) × Mo17	Self-pollinated	11	218	229	4.8[a]
6	*psc*(B73) × Mo17	Self-pollinated	17	227	244	7.0[a]
Total			58	935	993	5.8[a]
1	*psc*(B73) × Mo17	*psc*(B73)	14	33	47	29.8[b]
2	*psc*(B73) × Mo17	*psc*(B73)	22	59	81	27.2[b]
3	*psc*(B73) × Mo17	*psc*(B73)	37	124	161	23.0[b]
4	*psc*(B73) × Mo17	*psc*(B73)	33	116	149	22.1[b]
5	*psc*(B73) × Mo17	*psc*(B73)	31	129	160	19.4[b]
6	*psc*(B73) × Mo17	*psc*(B73)	15	38	53	28.3[b]
7	*psc*(B73) × Mo17	*psc*(B73)	34	116	150	22.7[b]
8	*psc*(B73) × Mo17	*psc*(B73)	50	166	216	23.1[b]
Total			236	781	1017	23.2[b]
1	*psc*(B73) × A188	*psc*(B73)	22	78	100	22.0[b]
2	*psc*(B73) × A188	*psc*(B73)	15	65	80	18.8[b]
Total			37	143	180	20.5[b]
1	*psc*(B73) × W22	*psc*(B73)	27	84	111	24.3[b]
2	*psc*(B73) × W22	*psc*(B73)	32	73	105	30.5[b]
Total			59	157	216	27.3[b]

[a] χ^2 values fail to reject the null hypothesis of a 15:1 segregation ratio, but reject a 3:1 ratio.
[b] χ^2 values fail to reject the null hypothesis of a 3:1 segregation ratio, but reject a 1:1 ratio.

TABLE 3

Carbohydrate levels, photosynthetic parameters, and chlorophyll content in wild-type and *psc* mutant plants

Parameter	Wild type	*psc* green	*psc* chlorotic
Sucrose[a]	18.54 ± 0.99	22.67 ± 2.13	43.54* ± 1.15
Glucose[a]	0.39 ± 0.05	0.43 ± 0.09	3.60* ± 0.16
Fructose[a]	0.80 ± 0.03	0.92 ± 0.14	2.18* ± 0.39
Starch[a]	23.65 ± 2.23	22.07 ± 2.45	41.33* ± 3.34
Photosynthetic rate[b]	41.78 ± 1.73	40.63 ± 1.30	1.70* ± 0.28
Stomatal conductance[b]	0.196 ± 0.01	0.20 ± 0.01	0.017* ± 0.004
Chlorophyll content[c]	51.3 ± 2.6	51.6 ± 2.6	16.1* ± 3.7

*Significantly different from wild type at $P \leq 0.05$ using Student's *t*-test.

[a] Data represent means of six samples ± the standard error. Units are mg per g fresh weight. Tissue was collected from summer nursery grown material at 8 pm.

[b] Data represent means of six samples ± the standard error. Units for photosynthesis rate are μmol CO_2 fixed m^{-2} s^{-1} and units for stomatal conductance measurements are μmol.

[c] Chlorophyll content (N = 25) is expressed in relative units.

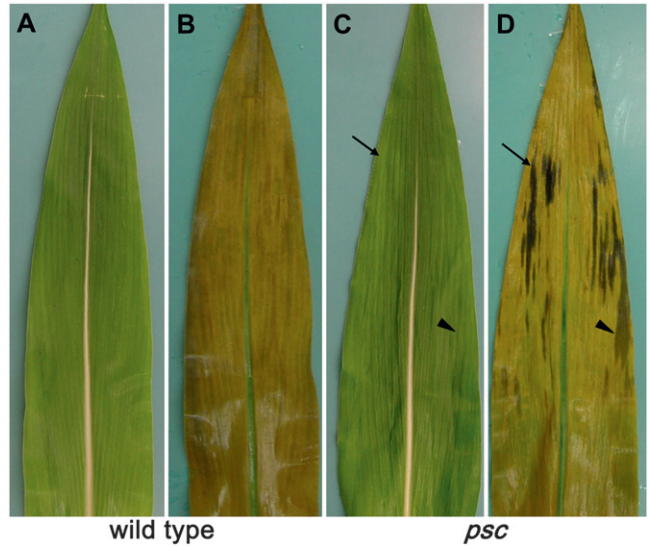

FIGURE 2.—Starch accumulation precedes chlorosis in *psc* mutant leaves. (A and C) Leaf photographs. (B and D) Same leaves cleared and IKI stained. (A and B) Wild type. (C and D) *psc* mutant. Arrow points to a region in a *psc* mutant leaf that has hyperaccumulated starch and progressed to chlorosis, whereas the arrowhead shows a region that has begun to hyperaccumulate starch but has not yet progressed to chlorosis.

Sugars have been demonstrated to repress photosynthetic gene expression and chlorophyll abundance in maize and other plants (SHEEN 1990; GOLDSCHMIDT and HUBER 1992; SHEEN 1994; KRAPP and STITT 1995; KOCH 1996; JEANNETTE *et al.* 2000). Because of the high sugar levels in *psc* chlorotic leaf tissues, we investigated the photosynthetic capacity of mutant and wild-type leaves. Green tissues in *psc* leaves had chlorophyll levels, photosynthesis, and stomatal conductance rates similar to wild type (Table 3). However, the chlorotic regions displayed photosynthesis and gas exchange rates of only 4–9% of those observed in wild type (Table 3). Additionally, *psc* chlorotic tissues had ~31% of the chlorophyll detected in the green tissues of *psc* or wild-type leaves. Hence, the excess accumulation of photoassimilates in *psc* chlorotic regions correlated with a downregulation of photosynthesis, decreased chlorophyll levels, and the closure of stomata.

Starch accumulation precedes chlorosis in developing *psc* leaves: In the *tdy1* and *tdy2* mutants, starch hyperaccumulation precedes formation of chlorotic tissues (BRAUN *et al.* 2006; BAKER and BRAUN 2008). To investigate whether carbohydrate accumulation also preceded chlorosis in *psc* leaves, we examined *psc* mutant and wild-type leaves in the process of emerging from the whorl. Developing leaves of *psc* mutants displayed chlorotic regions toward the mature tip of the leaves, but lacked chlorotic regions toward the immature leaf base (Figure 2, A and C). To inspect carbohydrate accumulation, we stained the leaves with IKI to monitor starch deposition. Wild-type leaves showed uniform, pale coloration and lacked any differential starch accumulation (Figure 2B). As expected, visible chlorotic regions within *psc* leaves showed strong starch staining (Figure 2D). However, the middle portion of *psc* leaves showed starch accumulation but did not display any observable difference in chlorophyll content (Figure 2C). These data imply that the visible chlorosis evident in *psc* mutant leaves is not directly due to defective chloroplasts, which accumulate excess carbohydrates. Instead, they suggest that the buildup of carbohydrates leads to the downregulation of chlorophyll accumulation in leaf tissues.

Chlorotic tissue boundaries are fixed and do not expand: The chlorotic phenotype of *psc* mutant leaves appears soon after leaves emerge from the whorl and after carbohydrates have begun to accumulate in discrete regions. To determine whether increased accumulation of carbohydrates resulted in the progressive expansion of chlorotic tissue, as seen in *sxd1* mutant leaves (RUSSIN *et al.* 1996), we monitored the formation of a *psc* chlorotic region over time. One day after a leaf began emerging from the whorl it had a uniform, pale-green appearance and no chlorosis was visible (data not shown). Two days after leaf emergence commenced, chlorotic regions first appeared (Figure 3A). Visible chlorotic regions were outlined to mark their boundaries and thereby follow their development. Seven days after emergence, the leaf tip had fully matured. The chlorotic tissue had not increased in relative size as indicated by the black outline appearing coincident with the boundary between green and chlorotic tissues (Figure 3B). Continuing to monitor the leaf for 10 additional days showed that the boundary was stable

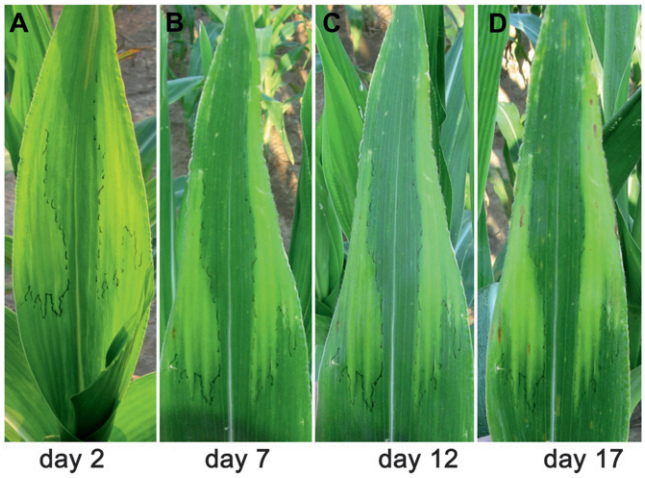

Figure 3.—The *psc* chlorotic leaf phenotype does not progressively expand. Photographs of the same *psc* mutant leaf over time. (A) Two days after leaf emergence. (B) Day 7. (C) Day 12. (D) Day 17.

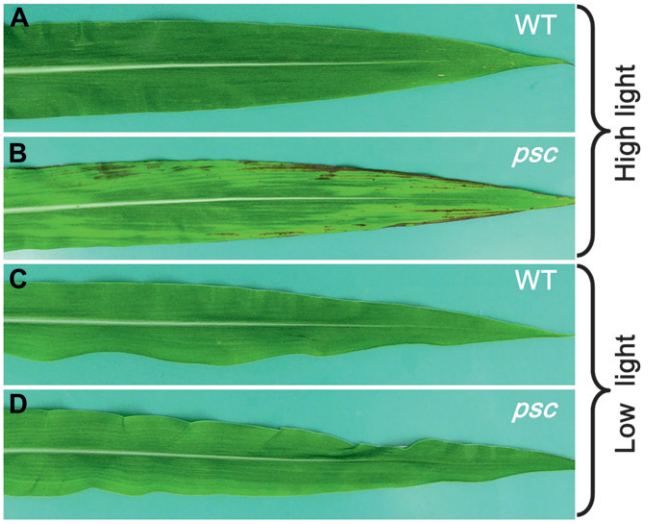

Figure 4.—High light is required for *psc* chlorotic tissue formation. (A and C) Wild type (WT). (B and D) *psc* mutant. (A and B) Leaves from plants grown under 2100 μmol m^{-2} sec^{-1} light. (C and D) Leaves from plants grown under 400 μmol m^{-2} sec^{-1} light.

(Figure 3, C and D). Hence, we propose that the formation of a *psc* chlorotic region occurs soon after leaf emergence, and that the tissue boundaries in mature leaves are permanent once formed, similar to *tdy1* and *tdy2* (Braun *et al.* 2006; Baker and Braun 2008).

High light induces the *psc* chlorotic phenotype: Expression of the *tdy* mutants chlorotic phenotype and the hyperaccumulation of carbohydrates require growth under high light (Braun *et al.* 2006; Baker and Braun 2008). To test whether light intensity influenced *psc* phenotypic expression, we grew wild-type and *psc* mutant plants in high- or low-light growth conditions. In high light, strong chlorotic regions were evident in *psc* leaves, whereas wild-type leaves appeared uniformly green (Figure 4, A and B). However, in low light, no chlorotic regions were visible in *psc* or wild-type leaves (Figure 4, C and D). These data suggest that high light is required to induce the *psc* phenotype, consistent with the idea that high rates of carbon assimilation underlie the formation of *psc* chlorotic leaf regions.

Veins are frequently found at *psc* tissue boundaries: Similar to the *tdy* mutants (Baker and Braun 2007, 2008), the boundaries between the different *psc* leaf phenotypic regions are often sharp (Figure 5A). To ascertain the nature of these boundaries and what may limit the expansion of a chlorotic region, we histologically examined these tissues for morphological features. In the proximal–distal axis of the leaf, no obvious morphological landmarks were found at the tissue boundaries. However, along the midrib–margin axis, ~70% of the distinct boundaries between *psc* green and chlorotic tissues occurred at large veins (Table 4). To determine whether the carbohydrate hyperaccumulation phenotype likewise showed a discrete boundary between chlorotic and green tissues, we analyzed leaf cross-sections from tissues harvested at the end of the night. Staining with IKI revealed that the boundary for both the tissue and starch accumulation phenotypes occurred at the large vein; *psc* chlorotic regions on one side of the vein contained abundant starch in the bundle sheath cells, whereas the green tissues on the other side of the vein had only trace amounts of starch (Figure 5B). In addition to large veins, 22% of the sharp boundaries between chlorotic and green tissue occurred at intermediate veins (Table 4). Starch staining revealed that the intermediate vein was also the boundary between greatly different levels of carbohydrates in the two tissues (Figure 5C). Intriguingly, for both the large and intermediate vein boundaries, chlorotic tissue adjacent to green tissue contained less starch than chlorotic tissue far from the tissue boundary (compare Figure 5, B and C with Figure 1G). Indeed, a gradual increase in starch accumulation in bundle sheath and mesophyll cells could be observed as the distance from the tissue boundary increased (Figure 5, D and E). Therefore, we infer that translocation of a mobile compound through the veins may influence the tissue phenotype.

Carbohydrate retention in *psc* leaves is correlated with decreased plant growth and yield: *tdy* and *sxd1* mutant plants show decreased growth and yield (Russin *et al.* 1996; Braun *et al.* 2006; Baker and Braun 2008; Ma *et al.* 2008). Because *psc* mutant leaves retain large amounts of carbohydrates, we hypothesized that less sucrose would be delivered to developing tissues and result in reduced plant growth and development. To assess this idea, we quantified plant height, leaf production, time to flowering, and reproductive traits. At maturity, *psc* mutant plants were ~12% shorter than wild type and produced about two fewer leaves (Figure 6A;

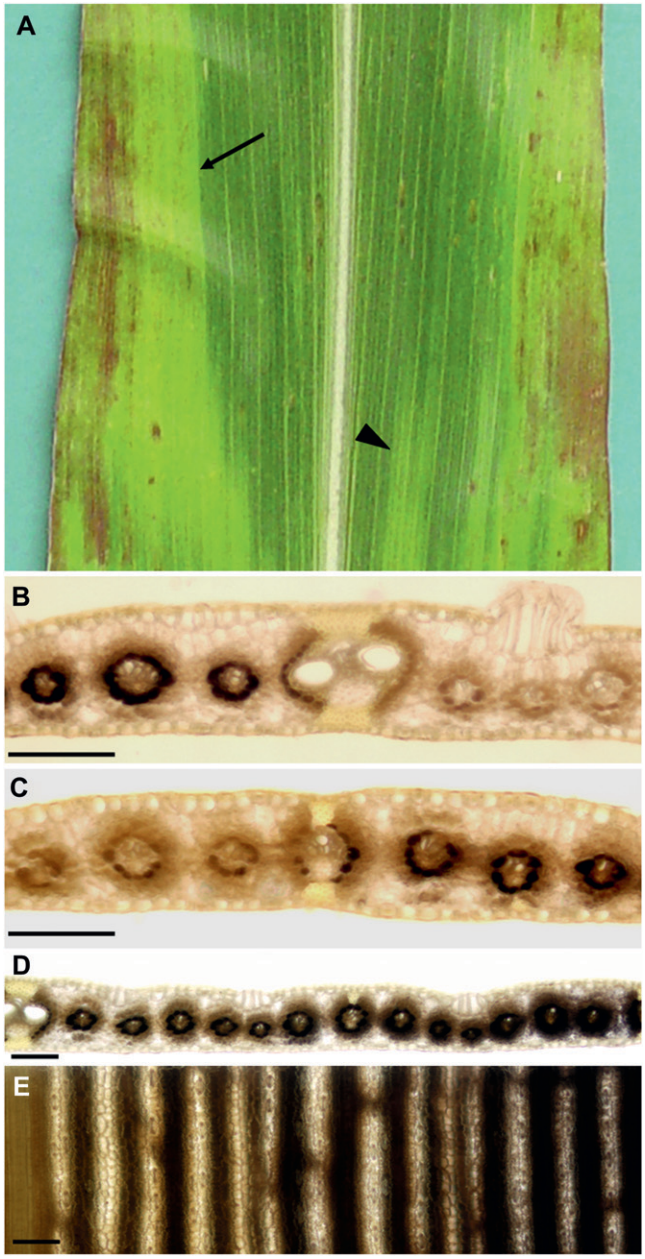

FIGURE 5.—Large and intermediate veins frequently delineate the boundary between *psc* chlorotic and green tissue. (A) *psc* mutant leaf showing a chlorotic and green tissue boundary at a large vein (arrow) as well as at an intermediate vein (arrowhead). (B) Cleared and IKI-stained cross-section of the boundary between chlorotic and green tissues marked with an arrow in A revealed it is located at a large vein. (C) Cleared and IKI-stained cross-section of the boundary between chlorotic and green tissues indicated with an arrowhead in A revealed it is located at an intermediate vein. (D) Lower magnification view of a cleared and IKI-stained cross-section of a chlorotic-green tissue boundary located at a large vein (left). (E) Abaxial view of D. In D and E, note the gradient of starch accumulation progressing into the chlorotic tissue (right). Bars, 100 μm.

Table 5). *psc* mutants also displayed a number of reproductive defects. The mutants were ~4 days delayed in pollen shed and in producing silks relative to wild type (Table 5). The mutants also showed an ~25% reduction

TABLE 4

***psc* chlorotic tissue boundary analysis**

Boundary location	%
Large vein	72
Intermediate vein	22
Other	6

Twenty leaves were used for the analysis and 5 randomly selected, distinct tissue boundaries were analyzed per leaf.

Other refers to no distinguishable feature identified at tissue boundary.

in ear length, tassel length, and kernel number, and an ~40% decrease in tassel branch number compared to wild type (Figure 6, B and C; Table 5). Additionally, the average kernel weight was reduced 18% in *psc* mutants. All of these phenotypes are consistent with carbohydrate retention within leaf tissues, which results in the failure to export enough sugars to sustain the growth of developing organs (Russin *et al.* 1996; Blauth *et al.* 2001; Niittyla *et al.* 2004; Braun *et al.* 2006; Baker and Braun 2008; Slewinski *et al.* 2009).

***Psc* functions independently of *Tdy1*, *Tdy2* and *Sxd1*:** To determine whether *Psc* might function in the same genetic pathway as either the *Tdy* or *Sxd1* genes, we generated double mutant families in the B73 background that segregated for *psc* and each of the other single mutants. In all F_2 families, the *psc* mutation segregated independently from *tdy1*, *tdy2*, and *sxd1*, in each case exhibiting a segregation ratio that conformed

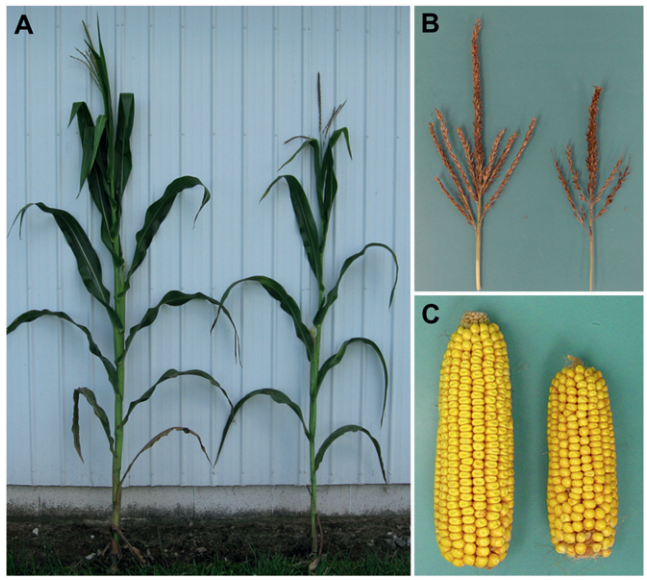

FIGURE 6.—*psc* mutants have reduced growth of vegetative and reproductive tissues. (A) Photograph of mature *psc* (right) and wild-type sibling (left) field grown plants. (B) *psc* tassels (right) display diminished growth compared to wild-type tassels (left). (C) *psc* ears (right) display reduced size and yield compared to wild-type ears (left).

TABLE 5

***psc* mutant plants have altered growth**

Growth parameters	Wild type	*psc* mutant	% WT
Plant height (cm)	208.8 ± 2.4	184.3* ± 3.9	88.3
Leaf number	20.9 ± 0.2	19.1* ± 0.3	91.2
Days to anthesis	79.0 ± 0.3	82.8* ± 0.6	104.8
Days to silking	79.8 ± 0.4	84.1* ± 0.7	105.2
Kernel weight (mg)	18.1 ± 0.6	14.9* ± 0.6	82.3
Kernel number	589.3 ± 16.5	439.5* ± 14.5	74.6
Ear length (cm)	14.3 ± 0.3	10.8* ± 0.3	75.5
Tassel length (cm)	39.9 ± 1.0	28.5* ± 1.1	71.4
Tassel branch number	7.0 ± 0.1	4.1* ± 0.7	58.6

Values are the means ± the standard error. ($N = 12$) WT, wild type. Kernel weight is the average of 100 kernels. *Significantly different from wild type at $P \leq 0.05$ using Student's *t*-test.

TABLE 6

Segregation data for *psc* and *tdy1* F_2 families

Family no.	WT	*psc*	*tdy1*	*psc; tdy1*	Total	χ^2	Probability
1	19	8	6	2	35	0.40	$P > 0.05$
2	26	11	15	4	56	2.98	$P > 0.05$
3	12	7	7	2	28	2.10	$P > 0.05$
4	11	9	6	1	27	4.67	$P > 0.05$
5	30	12	9	3	54	0.52	$P > 0.05$
6	27	7	10	2	46	0.84	$P > 0.05$
Total	125	54	53	14	246	3.79	$P > 0.05$

χ^2 analyses of *psc* and *tdy1* segregating in six F2 families fail to reject a 9:3:3:1 expectation. WT, wild type.

to a 9:3:3:1 expectation (Table 6; supporting information, Table S1). These data support the findings from the complementation tests, indicating that the *psc* mutation defines different genes than those previously identified to function in carbohydrate partitioning in maize. Furthermore, these data indicate that *Psc* shows no epistatic relationships with *Tdy1*, *Tdy2*, or *Sxd1*.

To investigate potential genetic interactions between *psc* and the *tdy* and *sxd1* mutants, we characterized the F_2 families for plant growth and time to reproductive maturity. At the whole-plant level, *psc* and *tdy1* single mutants were 10–12% shorter than wild-type siblings (Figure 7A; Table 7), whereas the *psc; tdy1* double mutant plants were 25% shorter than wild type. Similarly, both *psc* and *tdy1* single mutants each flowered ~5 days later than wild type, while the double mutant was twice as slow to shed pollen or extrude silks (Table 7). Hence, the *psc; tdy1* double mutants displayed approximately double the phenotypic severity in plant height and time to flowering compared with the single mutants, suggesting an additive genetic interaction.

To test this hypothesis, we analyzed leaf chlorosis and starch accumulation in the F_2 plants. Leaves of the *psc; tdy1* double mutant exhibited a greater percentage of chlorotic tissues compared to either the *psc* or *tdy1* single mutants, but still contained some distinct green regions (Figure 7B). Double mutant leaves also accumulated significantly more anthocyanins than the single mutants. Anthocyanins have been shown to accumulate in tissues containing high levels of carbohydrates that are experiencing osmotic stress (Russin *et al.* 1996; Chalker-Scott 1999; Baker and Braun 2007). IKI-staining the leaves confirmed that all of the chlorotic tissue contained excess starch, whereas the green regions of the single and double mutants appeared similar to wild type (Figure 7C). Within the double mutant leaves, the two single mutant variegation patterns appeared to independently overlay one another. Some leaf areas displayed the streaked, longitudinal chlorosis associated with the *psc* mutant phenotype (Figure 7D, arrow), while other regions showed the distinctive appearance of a *tdy1* chlorotic region (Figure 7D, arrowhead). Moreover, there were regions in which the two distinct variegation patterns overlapped. Leaf regions expressing both mutant phenotypes exhibited more severe chlorosis than either single mutant (Figure 7D, asterisk). This strongly chlorotic tissue was visible before, accumulated anthocyanins earlier, and progressed to necrosis sooner than adjacent leaf tissue expressing only one of the chlorotic mutant phenotypes (data not shown). Hence, the leaf chlorosis and excess starch phenotypes in the double mutant leaves appeared to result from the independent expression of each single mutant phenotype, suggesting that *Psc* and *Tdy1* function in separate genetic pathways.

Similar analyses with *tdy2* and *sxd1* suggest that *Psc* function is independent of previously defined pathways regulating carbohydrate partitioning in maize (Figure S1, Table S1, and Table S2). In support of this, *psc* mutants did not exhibit ectopic callose deposits at the bundle sheath–vascular parenchyma cell interface, which are present in *sxd1* mutants, and did not influence this phenotype in the *psc; sxd1* double mutant leaves (Figure S2) (Botha *et al.* 2000; Baker and Braun 2008; Ma *et al.* 2008).

DISCUSSION

We have taken a genetic approach to identify genes that promote carbon export from maize leaves. Previously, three variegated maize mutants, *sxd1*, *tdy1*, and *tdy2* have been implicated as defective in carbon movement out of leaves. In this report, we describe a new mutant, *psc*, which hyperaccumulates carbohydrates within discrete chlorotic leaf regions. By characterizing the *psc* mutant phenotype and its genetic interaction with the other variegation mutants that accumulate excess carbohydrates, we determined that *psc* defines a new pair of redundantly acting genes regulating carbohydrate partitioning in maize.

Redundant genetic functions may be common in maize, as it is an ancient segmental allotetraploid with

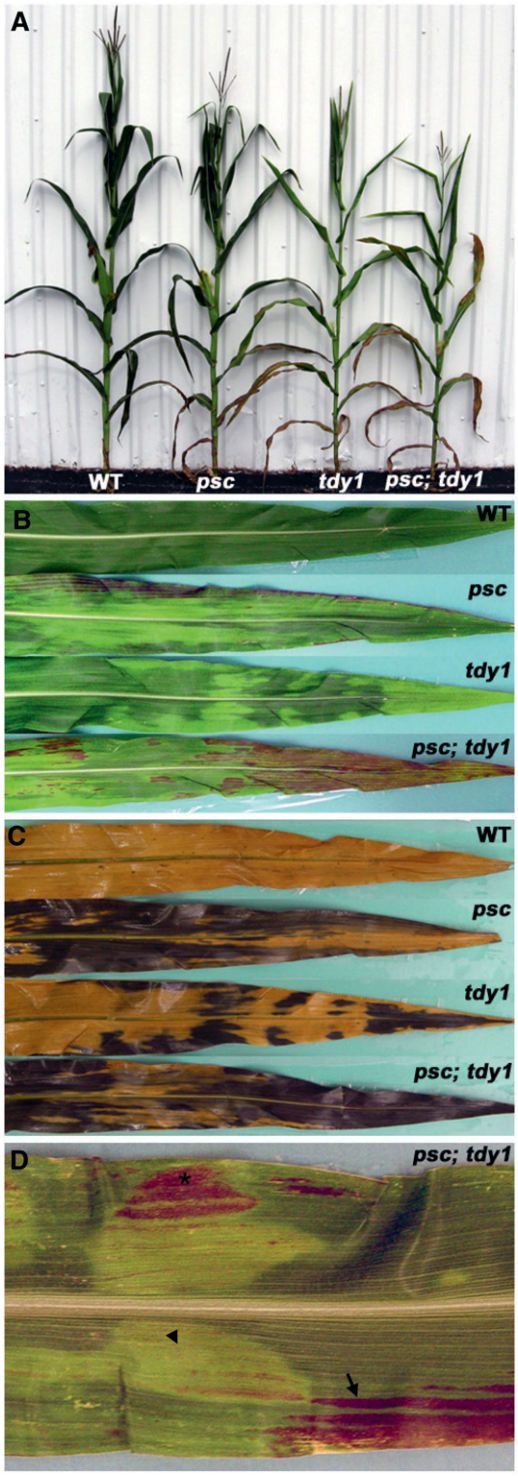

Figure 7.—*psc* and *tdy1* exhibit an additive genetic interaction. (A) Photograph of mature wild-type (WT), *psc*, *tdy1*, and *psc; tdy1* double mutant plants. (B) Leaves from wild type, *psc*, *tdy1*, and *psc; tdy1* double mutants. (C) Same leaves as shown in B, cleared and IKI stained. (D) Close-up of overlapping *tdy1* and *psc* chlorotic tissues from a *psc; tdy1* double mutant. Arrow indicates longitudinally streaked *psc* chlorotic tissue accumulating anthocyanins. Arrowhead indicates *tdy1* chlorotic region. Asterisk indicates severely chlorotic tissue expressing both the *psc* and *tdy1* chlorotic phenotypes and accumulating anthocyanins.

multiple duplicated, colinear chromosomal regions (Gaut and Doebley 1997). Previous studies found functional redundancy for maize genes that map to homeologous chromosomal positions (Rhoades 1951; Coe *et al.* 1981; Wright *et al.* 1992; Mena *et al.* 1996; Scanlon *et al.* 1996), indicating that the duplicated genes have identical or partially overlapping functions. For the later cases, these are likely caused by subfunctionalization, resulting in diverging tissue-specific expression patterns (Lynch and Force 2000; Langham *et al.* 2004). Indeed, recent analyses of the maize genome revealed hundreds of variants for gene copy number as well as thousands of present–absent variants between the B73 and Mo17 inbred lines (Schnable *et al.* 2009; Springer *et al.* 2009). These haplotype-specific sequences likely contribute to the tremendous phenotypic diversity present in maize and may explain differences in inheritance patterns of mutations observed in different maize inbred lines.

***Psc* promotes carbohydrate export from maize leaves:** Hyperaccumulation of starch in the mesophyll cells of C_4 plants is only observed when carbon export is severely perturbed. Physiological disruptions leading to this phenotype include removing developing ears from adult plants (Allison and Weinmann 1970) or inhibiting phloem transport by techniques such as girdling (Goldschmidt and Huber 1992; Krapp and Stitt 1995; Jeannette *et al.* 2000; Slewinski *et al.* 2009). The *psc*, *sxd1*, *tdy1*, and *tdy2* mutants all display carbohydrate hyperaccumulation in both bundle sheath and mesophyll cells within chlorotic leaf regions. Therefore, this indicates that they are defective in carbon export from leaves (Russin *et al.* 1996; Braun *et al.* 2006; Baker and Braun 2008; Slewinski *et al.* 2009).

Similar to the *tdy* mutants, high light is needed to generate the *psc* variegation phenotype. When grown under high-light conditions, *psc* mutant leaves exhibit stable, chlorotic regions that are first visible 2 days postemergence from the whorl. These chlorotic tissues form only during a limited developmental period as the leaf emerges and remain fixed throughout the life of the leaf. On the basis of these data, we hypothesize that the buildup of a photosynthetic byproduct in high light, for example sucrose, triggers *psc* chlorotic tissue formation during leaf development. Once leaf maturation progresses beyond a developmental time point, the *psc* mutant phenotype is irreversible. Thus, *Psc* is predicted to act at or prior to the time when the mutant phenotype is first detectable, potentially when the leaves are still immature sink tissues (Evert *et al.* 1996).

Larger order veins are implicated in *psc* chlorotic tissue formation. In the lateral dimension, 94% of the *psc* chlorotic region boundaries occurred at large or intermediate veins, suggesting that these veins limit the movement of the chlorotic-tissue-inducing compound. This may also account for the longitudinally streaked

TABLE 7

Growth parameters of *psc; tdy1* double mutants

Phenotype	Plant height (cm)	% WT	Days to anthesis	% WT	Days to silking	% WT
Wild type	237.8 ± 0.2	100	85.2 ± 0.1	100	86.1 ± 0.1	100
psc	216.7* ± 0.4	91.1	89.6* ± 0.1	105.2	91.6** ± 0.1	106.4
tdy1	209.7* ± 0.6	88.1	89.9* ± 0.1	105.4	91.5* ± 0.1	106.2
psc; tdy1	177.4** ± 2.6	74.6	94.3** ± 0.3	110.7	96.3** ± 0.3	111.8

Values are the means ± standard error. N = 40 for wild type (WT), 25 *psc*, 26 *tdy1*, and 6 *psc; tdy1*. *Significantly different from wild type at $P \leq 0.05$ using Student's *t*-test. **Significantly different from wild type, *psc* and *tdy1* single mutants at $P \leq 0.05$ using Student's *t*-test.

nature of the phenotype. In comparison, only 68–74% of the sharp tissue boundaries occurred at large and intermediate veins in *tdy1* and *tdy2* leaves (Baker and Braun 2007, 2008). Hypodermal sclerenchyma caps are present in both intermediate and large, but not small, veins (Russell and Evert 1985). Hence, these may function as barriers to restrict the diffusion of solutes in the apoplast and underlie the formation of a sharp boundary between chlorotic and green tissues. The sharp boundaries at these veins suggest that *Psc* may function to promote the long-distance translocation of sucrose within the phloem. Alternative possibilities are that *Psc* functions to induce sucrose export to the phloem or to sequester sugars in the vacuole and/or chloroplast, when excess levels of these substances are generated in high-light environments.

A threshold model to explain the variegation pattern of chlorosis as proposed for the *tdy* loci may also apply to *psc* (Braun *et al.* 2006; Baker and Braun 2008). In brief, the determination of leaf tissue to form a chlorotic region is based on a threshold of sucrose or other chloroplast byproduct which is experienced during a limited developmental window during leaf emergence. If the threshold is surpassed, a chlorotic region will form. If the concentration of this signal remains below the threshold, the tissue will mature to form normal green tissue. Vascular tissue may act to attenuate, export, or detoxify this signal, thus drastically reducing its concentration when large or intermediate veins are encountered. This may explain the observation that most chlorotic-green region boundaries occur at these veins.

Retention of carbohydrates and reduction in photosynthetic capacity are associated with a significant decrease in vegetative and reproductive growth in *psc* mutants. A decrease in vegetative growth is manifested as a reduction in plant height, whereas a decrease in reproductive growth is observed as reduced tassel size and branching, ear length, and time to flowering. Kernel number and mass are also significantly decreased in the *psc* mutant. These data suggest that *Psc* may play a role in maintaining a proper balance between carbohydrate assimilation, compartmentation, export, transport, or import within the developing maize plant.

The hyperaccumulation of carbohydrates within the chlorotic leaf regions may be caused by the import of carbohydrates from the surrounding green tissue. Alternatively, *psc* chlorotic tissue may result from a severe defect in carbon export. Support for the second possibility comes from the following observation: *psc* chlorotic tissue located directly adjacent to green tissue displays a reduced starch hyperaccumulation phenotype compared to *psc* chlorotic tissue further from the vein boundary. This starch accumulation pattern is the opposite of what would be predicted if *psc* chlorotic regions were importing carbohydrates from green tissues. The gradient in starch levels can be explained by a compensatory export affect from the green tissue, which presumably maintains normal export function and thereby siphons excess carbohydrates from the chlorotic tissue at the boundary. These data suggest that *psc* chlorotic tissues are impaired in carbohydrate transport, resulting in the overaccumulation of starch and sugars. Hence, we propose that *Psc* functions to promote carbohydrate export from maize leaves.

Although the *psc* mutant phenotype resembles those of the *sxd1* and *tdy* mutants in displaying leaf variegation and carbohydrate retention, it is distinct from them in several ways. For instance, in *sxd1* mutant leaves, the phenotype becomes progressively more chlorotic as the leaf ages (Russin *et al.* 1996), leading to premature leaf senescence, which is not observed in the *psc* mutants. Additionally, in *sxd1* leaves, carbon export is blocked by ectopic callose deposition over the plasmodesmata at the bundle sheath–vascular parenchyma cell interface of minor veins (Botha *et al.* 2000), a phenotype not detected in *psc* mutants. An additive genetic interaction between *psc* and *sxd1* suggests that *Psc* acts in a distinct pathway contributing to carbohydrate partitioning in maize leaves.

Both the *psc* and *tdy* mutants require high light to induce leaf chlorosis; however, the leaf variegation patterns are distinct. In contrast to the *tdy* mutants, *psc* mutants chlorotic regions appear longitudinally streaked and tend to be located near the leaf margins. These differences suggest that the *psc* and *tdy* mutant phenotypes are caused by divergent processes, such as different sensitivities to developmental timing, position within the leaf, light perception, signal transduction, and/or response. This hypothesis is supported by the variegation phenotype observed in *psc; tdy* double

mutant leaves, wherein *psc* and *tdy* chlorotic tissues form independently of each other. Therefore, these data are consistent with the assertion that *Psc* and the *Tdy* genes function in separate genetic pathways.

Additive genetic interactions between *psc* and the *tdy* mutants in leaf variegation, plant growth, and reproductive traits suggest that *Psc* function is unrelated to the *Tdy* pathway. However, it cannot be excluded that *psc* is a hypomorphic rather than null mutation. If so, it could complicate the interpretation of the genetic interaction experiments. One method to determine the nature of mutant alleles in maize is to perform a dosage analysis (Muller 1932; Birchler 1994); however, the duplicate-factor recessive inheritance of the *psc* mutation hampers such an analysis. Nonetheless, our characterization of the *psc* mutant phenotype identifies a new genetic function that when disrupted leads to carbohydrate partitioning defects in maize.

In conclusion, characterization of the *psc* mutant phenotype and genetic analyses with similar carbohydrate accumulating mutants of maize suggest that the wild-type *Psc* genes act independently of previously identified genetic pathways. Future work to clone and characterize the *Psc* genes will elucidate how they redundantly function and contribute to the complex regulation of carbohydrate partitioning in higher plants.

We thank Tony Omeis and Scott Harkcom for excellent plant care and Sally Assmann for the use of the LICOR 6400. We thank two reviewers for improvements and the members of the Braun and McSteen labs for discussion of the data and comments on the manuscript. This work was supported by the National Research Initiative of the United States Department of Agriculture Cooperative State Research, Education and Extension Service, grant number 2008-35304-04597 (to D.M.B.).

LITERATURE CITED

Allison, J. C. S., and H. Weinmann, 1970 Effect of absence of developing grain on carbohydrate content and senescence of maize leaves. Plant Physiol. **46:** 435–436.

Baker, R. F., and D. M. Braun, 2007 *tie-dyed1* functions non-cell autonomously to control carbohydrate accumulation in maize leaves. Plant Physiol. **144:** 867–878.

Baker, R. F., and D. M. Braun, 2008 *tie-dyed2* functions with *tie-dyed1* to promote carbohydrate export from maize leaves. Plant Physiol. **146:** 1085–1097.

Birchler, J., 1994 Dosage analysis using B-A translocations, pp. 328–329 in *The Maize Handbook*, edited by M. Freeling and V. Walbot. Springer-Verlag, New York.

Blauth, S., Y. Yao, J. Klucinec, J. Shannon, D. Thompson *et al.*, 2001 Identification of *Mutator* insertional mutants of starch-branching enzyme 2a in corn. Plant Physiol. **125:** 1396–1405.

Botha, C. E. J., R. H. M. Cross, A. J. E. van Bel and C. I. Peter, 2000 Phloem loading in the sucrose-export-defective (SXD-1) mutant maize is limited by callose deposition at plasmodesmata in bundle sheath-vascular parenchyma interface. Protoplasma **214:** 65–72.

Braun, D. M., Y. Ma, N. Inada, M. G. Muszynski and R. F. Baker, 2006 *tie-dyed1* regulates carbohydrate accumulation in maize leaves. Plant Physiol. **142:** 1511–1522.

Braun, D. M., and T. L. Slewinski, 2009 Genetic control of carbon partitioning in grasses: roles of *Sucrose Transporters* and *Tie-dyed* loci in phloem loading. Plant Physiol. **149:** 71–81.

Chalker-Scott, L., 1999 Environmental significance of anthocyanins in plant stress responses. Photochem. Photobiol. **70:** 1–9.

Cheng, W. H., E. W. Taliercio and P. S. Chourey, 1996 The *Miniature1* seed locus of maize encodes a cell wall invertase required for normal development of endosperm and maternal cells in the pedicel. Plant Cell **8:** 971–983.

Chiou, T. J., and D. R. Bush, 1998 Sucrose is a signal molecule in assimilate partitioning. Proc. Natl. Acad. Sci. USA **95:** 4784–4788.

Coe, E. H., S. M. McCormick and S. A. Modena, 1981 White pollen in maize. J. Hered. **72:** 318–320.

Dinges, J. R., C. Colleoni, M. G. James and A. M. Myers, 2003 Mutational analysis of the pullulanase-type debranching enzyme of maize indicates multiple functions in starch metabolism. Plant Cell **15:** 666–680.

Edwards, G. E., V. R. Franceschi, M. S. B. Ku, E. V. Voznesenskaya, V. I. Pyankov *et al.*, 2001 Compartmentation of photosynthesis in cells and tissues of C_4 plants. J. Exp. Bot. **52:** 577–590.

Esau, K., 1977 *Anatomy of Seed Plants*. John Wiley & Sons, New York.

Evert, R. F., 1980 Vascular anatomy of angiospermous leaves, with special consideration of the maize leaf. Ber. Deutsch. Bot. Ges. **93:** 43–55.

Evert, R. F., W. Eschrich and W. Heyser, 1978 Leaf structure in relation to solute transport and phloem loading in *Zea mays* L. Planta **138:** 279–294.

Evert, R. F., W. A. Russin and A. M. Bosabalidis, 1996 Anatomical and ultrastructural changes associated with sink-to-source transition in developing maize leaves. Int. J. Plant Sci. **157:** 247–261.

Fritz, E., R. F. Evert and W. Heyser, 1983 Microautoradiographic studies of phloem loading and transport in the leaf of *Zea mays* L. Planta **159:** 193–206.

Fritz, E., R. F. Evert and H. Nasse, 1989 Loading and transport of assimilates in different maize leaf bundles: digital image analysis of ^{14}C microautoradiographs. Planta **178:** 1–9.

Gaut, B. S., and J. F. Doebley, 1997 DNA sequence evidence for the segmental allotetraploid origin of maize. Proc. Natl. Acad. Sci. USA **94:** 6809–6814.

Goldschmidt, E. E., and S. C. Huber, 1992 Regulation of photosynthesis by end-product accumulation in leaves of plants storing starch, sucrose, and hexose sugars. Plant Physiol. **99:** 1443–1448.

Hannah, L. C., 2005 Starch synthesis in the maize endosperm. Maydica **50:** 497–506.

Heyser, W., 1980 Phloem loading in the maize leaf. Ber. Deutsch. Bot. Ges. **93:** 221–228.

Heyser, W., R. F. Evert, E. Fritz and W. Eschrich, 1978 Sucrose in the free space of translocating maize leaf bundles. Plant Physiol. **62:** 491–494.

Hofstra, G., and C. Nelson, 1969 The translocation of photosynthetically assimilated ^{14}C in corn. Can. J. Bot. **47:** 1435–1442.

Huang, M., T. L. Slewinski, R. F. Baker, D. Janick-Buckner, B. Buckner *et al.*, 2009 Camouflage patterning in maize leaves results from a defect in porphobilinogen deaminase. Mol. Plant **2:** 773–789.

Jeannette, E., A. Reyss, N. Gregory, P. Gantet and J. L. Prioul, 2000 Carbohydrate metabolism in a heat-girdled maize source leaf. Plant Cell Environ. **23:** 61–69.

Kalt-Torres, W., P. S. Kerr, H. Usuda and S. C. Huber, 1987 Diurnal changes in maize leaf photosynthesis: I. Carbon exchange rate, assimilate export rate, and enzyme activities. Plant Physiol. **83:** 283–288.

Koch, K. E., 1996 Carbohydrate-modulated gene expression in plants. Annu. Rev. Plant Physiol. Plant Mol. Biol. **47:** 509–540.

Krapp, A., and M. Stitt, 1995 An evaluation of direct and indirect mechanisms for the "sink-regulation" of photosynthesis in spinach: changes in gas exchange, carbohydrates, metabolites, enzyme activities and steady-state transcript levels after cold-girdling source leaves. Planta **195:** 313–323.

Lalonde, S., D. Wipf and W. B. Frommer, 2004 Transport mechanisms for organic forms of carbon and nitrogen between source and sink. Annu. Rev. Plant Biol. **55:** 341–372.

Langham, R. J., J. Walsh, M. Dunn, C. Ko, S. A. Goff *et al.*, 2004 Genomic duplication, fractionation and the origin of regulatory novelty. Genetics **166:** 935–945.

Lu, Y., and T. D. Sharkey, 2004 The role of amylomaltase in maltose metabolism in the cytosol of photosynthetic cells. Planta **218:** 466–473.

Lunn, J. E., and R. T. Furbank, 1999 Tansley Review No. 105. Sucrose biosynthesis in C_4 plants. New Phytol. **143:** 221–237.

Lynch, M., and A. Force, 2000 The probability of duplicate gene preservation by subfunctionalization. Genetics **154:** 459–473.

Ma, Y., R. F. Baker, M. Magallanes-Lundback, D. DellaPenna and D. M. Braun, 2008 *Tie-dyed1* and *Sucrose export defective1* act independently to promote carbohydrate export from maize leaves. Planta **227:** 527–538.

Ma, Y., T. L. Slewinski, R. F. Baker and D. M. Braun, 2009 *Tie-dyed1* encodes a novel, phloem-expressed transmembrane protein that functions in carbohydrate partitioning. Plant Physiol. **149:** 181–194.

Mena, M., B. A. Ambrose, R. B. Meeley, S. P. Briggs, M. F. Yanofsky *et al.*, 1996 Diversification of C-function activity in maize flower development. Science **274:** 1537–1540.

Moore, B., L. Zhou, F. Rolland, Q. Hall, W. H. Cheng *et al.*, 2003 Role of the *Arabidopsis* glucose sensor HXK1 in nutrient, light, and hormonal signaling. Science **300:** 332–336.

Muller, H. J., 1932 Further studies on the nature and causes of gene mutations. Proceedings of the 6th International Congress of Genetics, Ithaca, NY, Vol. 1, pp. 213–255.

Niittyla, T., G. Messerli, M. Trevisan, J. Chen, A. M. Smith *et al.*, 2004 A previously unknown maltose transporter essential for starch degradation in leaves. Science **303:** 87–89.

Nolte, K. D., and K. E. Koch, 1993 Companion-cell specific localization of sucrose synthase in zones of phloem loading and unloading. Plant Physiol. **101:** 899–905.

Poethig, R. S., and E. J. Szymkowiak, 1995 Clonal analysis of leaf development in maize. Maydica **40:** 67–76.

Provencher, L. M., L. Miao, N. Sinha and W. J. Lucas, 2001 *Sucrose export defective1* encodes a novel protein implicated in chloroplast-to-nucleus signaling. Plant Cell **13:** 1127–1141.

Rhoades, M., and A. Carvalho, 1944 The function and structure of the parenchyma sheath plastids of the maize leaf. Bull. Torrey Bot. Club **71:** 335–346.

Rhoades, M. M., 1951 Duplicate genes in maize. Am. Nat. **85:** 105–110.

Russell, S. H., and R. F. Evert, 1985 Leaf vasculature in *Zea mays* L. Planta **164:** 448–458.

Russin, W. A., R. F. Evert, P. J. Vanderveer, T. D. Sharkey and S. P. Briggs, 1996 Modification of a specific class of plasmodesmata and loss of sucrose export ability in the *sucrose export defective1* maize mutant. Plant Cell **8:** 645–658.

Ruzin, S., 1999 *Plant Microtechnique and Microscopy*. Oxford University Press, New York.

Sattler, S. E., E. B. Cahoon, S. J. Coughlan and D. DellaPenna, 2003 Characterization of tocopherol cyclases from higher plants and cyanobacteria. Evolutionary implications for tocopherol synthesis and function. Plant Physiol. **132:** 2184–2195.

Sauer, N., 2007 Molecular physiology of higher plant sucrose transporters. FEBS Lett. **581:** 2309–2317.

Scanlon, M. J., R. G. Schneeberger and M. Freeling, 1996 The maize mutant *narrow sheath* fails to establish leaf margin identity in a meristematic domain. Development **122:** 1683–1691.

Schnable, P. S., D. Ware, R. S. Fulton, J. C. Stein, F. Wei *et al.*, 2009 The B73 maize genome: complexity, diversity, and dynamics. Science **326:** 1112–1115.

Sheen, J., 1990 Metabolic repression of transcription in higher plants. Plant Cell **2:** 1027–1038.

Sheen, J., 1994 Feedback-control of gene-expression. Photosynth. Res. **39:** 427–438.

Slewinski, T. L., and D. M. Braun, 2010 Current perspectives on the regulation of whole-plant carbohydrate partitioning. Plant Sci. **178:** 10.1016/j.plantsci.2010.1001.1010.

Slewinski, T. L., Y. Ma, R. F. Baker, M. Huang, R. Meeley *et al.*, 2008 Determining the role of *Tie-dyed1* in starch metabolism: epistasis analysis with a maize ADP-glucose pyrophosphorylase mutant lacking leaf starch. J. Hered. **99:** 661–666.

Slewinski, T. L., R. Meeley and D. M. Braun, 2009 *Sucrose transporter1* functions in phloem loading in maize leaves. J. Exp. Bot. **60:** 881–892.

Smith, A. M., and M. Stitt, 2007 Coordination of carbon supply and plant growth. Plant Cell Environ. **30:** 1126–1149.

Springer, N. M., K. Ying, Y. Fu, T. Ji, C.-T. Yeh *et al.*, 2009 Maize inbreds exhibit high levels of copy number variation (CNV) and presence/absence variation (PAV) in genome content. PLoS Genet. **5:** e1000734.

Srivastava, A. C., S. Ganesan, I. O. Ismail and B. G. Ayre, 2008 Functional characterization of the *Arabidopsis thaliana* AtSUC2 Suc/H^+ symporter by tissue-specific complementation reveals an essential role in phloem loading but not in long-distance transport. Plant Physiol. **147:** 200–211.

Stitt, M., R. M. Lilley, R. Gerhardt and H. W. Heldt, 1989 Metabolite levels in specific cells and subcellular compartments of plant leaves. Methods Enzymol. **174:** 518–552.

Turgeon, R., 2006 Phloem loading: how leaves gain their independence. BioScience **56:** 15–24.

Wardlaw, I. F., 1990 Tansley Review No. 27. The control of carbon partitioning in plants. New Phytol. **116:** 341–381.

Whitt, S. R., L. M. Wilson, M. I. Tenaillon, B. S. Gaut and E. S. Buckler, 2002 Genetic diversity and selection in the maize starch pathway. Proc. Natl. Acad. Sci. USA **99:** 12959–12962.

Wright, A. D., C. A. Moehlenkamp, G. H. Perrot, M. G. Neuffer and K. C. Cone, 1992 The maize auxotrophic mutant orange pericarp is defective in duplicate genes for tryptophan synthase beta. Plant Cell **4:** 711–719.

Zeeman, S., S. Smith and A. Smith, 2007 The diurnal metabolism of leaf starch. Biochem. J. **401:** 13–28.

Communicating editor: P. T. Brutnell

GENETICS

Supporting Information
http: //www.genetics.org/cgi/content/full/genetics.109.113357/DC1

The *Psychedelic* Genes of Maize Redundantly Promote Carbohydrate Export From Leaves

Thomas L. Slewinski and David M. Braun

DOI: 10.1534/genetics.109.113357

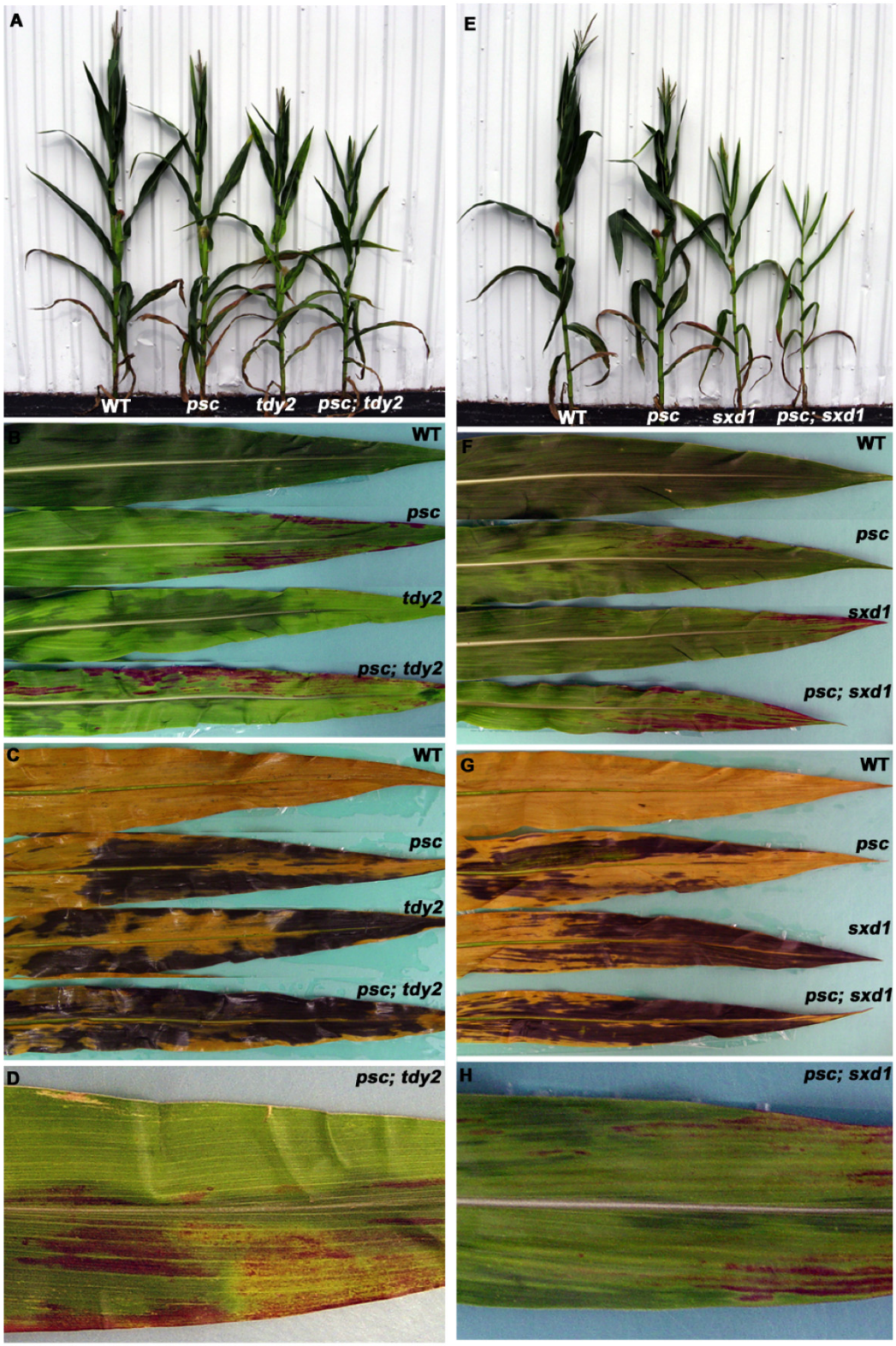

FIGURE S1.—*psc* exhibits an additive genetic interaction with *tdy2* or *sxd1*. (A) photograph of mature wild-type (WT), *psc*, *tdy2* and *psc; tdy2* double mutant plants. (B) leaves from wild type, *psc*, *tdy2* and *psc; tdy2* double mutants. (C) same leaves as shown in (B), cleared and IKI-stained. (D) close up of overlapping *tdy2* and *psc* chlorotic tissues from *psc; tdy2* double mutant. (E) photograph of mature wild-type, *psc*, *sxd1* and *psc; sxd1* double mutant plants. (F) leaves from wild type, *psc*, *sxd1* and *psc; sxd1* double mutants. (G) same leaves as shown in (F) cleared and IKI-stained. (H) close up of overlapping *sxd1* and *psc* chlorotic tissues from *psc; sxd1* double mutant.

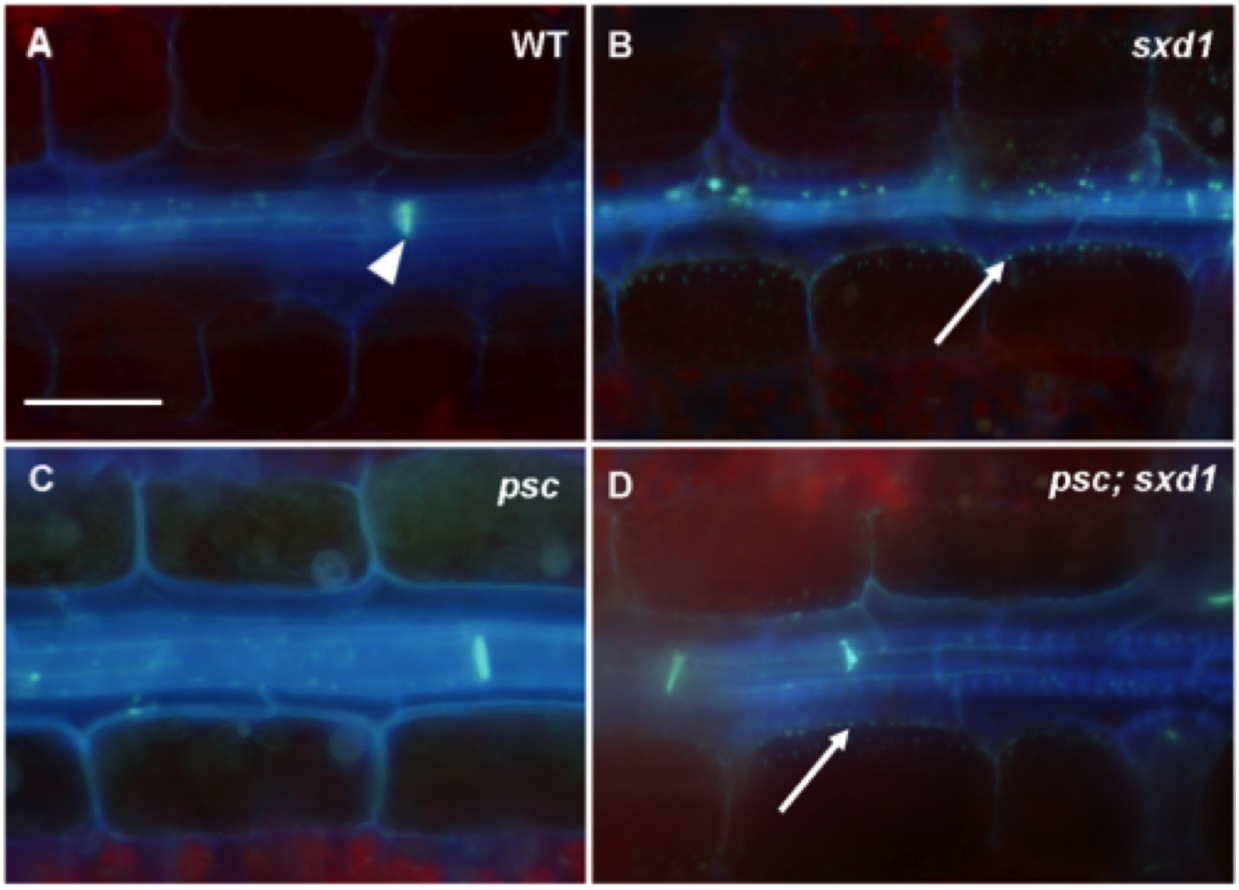

FIGURE S2.—Aniline blue staining of callose in wild type, *psc* and *sxd1* single and double mutant leaves. A-D, Paradermal sections of leaf minor veins examined under UV light. A, wild type (WT). Arrowhead indicates a sieve plate between sieve elements. B, *sxd1* mutant. C, *psc* mutant. D, *psc; sxd1* double mutant. Arrows indicate ectopic callose occlusions at the vascular parenchyma-bundle sheath cell interface. Scale bar = 50 mm for all panels.

TABLE S1

Segregation data for *psc* and *tdy2* and for *psc* and *sxd1* F2 families

Family #	wild type	*psc* mutant	single mutant	double mutant	Total	χ^2	Probability
psc; tdy2			*tdy2*				
1	19	10	6	3	38	1.77	$P > 0.05$
2	23	13	10	5	51	3.41	$P > 0.05$
3	25	12	9	2	48	1.48	$P > 0.05$
4	23	12	13	3	51	3.00	$P > 0.05$
5	26	6	9	2	43	0.95	$P > 0.05$
6	28	13	11	4	56	1.08	$P > 0.05$
Total	**144**	**66**	**58**	**19**	**287**	**5.03**	***P* > 0.05**
psc; sxd1			*sxd1*				
1	22	10	10	5	47	2.51	$P > 0.05$
2	19	14	13	3	49	6.76	$P > 0.05$
3	20	5	7	2	34	0.41	$P > 0.05$
4	25	11	12	4	52	1.47	$P > 0.05$
Total	**86**	**40**	**42**	**14**	**182**	**6.05**	***P* > 0.05**

χ^2 analyses fail to reject a 9: 3: 3: 1 expectation for all F2 families.

TABLE S2

Growth parameters in *psc; tdy2* and *psc; sxd1* segregating double mutant families

Phenotype	Plant height (cm)	% WT	Days to anthesis	% WT	Days to silking	% WT
wild type	237.2 ± 0.0	100	84.6 ± 0.3	100	86.3 ± 0.1	100
psc	226.1* ± 0.7	95.3	89.2* ± 0.3	105.4	89.2* ± 0.2	103.4
tdy2	214.3* ± 0.6	90.3	90.3* ± 0.2	107.2	91.0* ± 0.2	105.4
psc; tdy2	193.9** ± 1.3	81.7	94.3** ± 0.8	111.5	96.8** ± 1.0	112.1
wild type	250.0 ± 0.5	100	Nd		Nd	
psc	220.4* ± 1.4	88.2	Nd		Nd	
sxd1	186.8* ± 0.9	74.7	Nd		Nd	
psc; sxd1	130.4** ± 5.1	52.16	Nd		Nd	

Values are the means ± standard error. N = 40 for wild type (WT), 25 for single mutants and 6 for double mutants.
***** Indicates that value is significantly different from wild type at $P \leq 0.05$ using Student's *t*-test.
****** Indicates that value is significantly different from wild type and both respective single mutants at $P \leq 0.05$ using Student's *t*-test. Nd = not determined due to the failure of the double mutants to shed pollen or make silks.